THE JOURNAL OF PHYSICAL CHEMISTRY A
A JOURNAL OF THE AMERICAN CHEMICAL SOCIETY

pubs.acs.org/JPCA

Perspective

# A Perspective on the Simulation of Electronic Circular Dichroism and Circularly Polarized Luminescence Spectra in Chiral Solid Materials

Marco Caricato*

Cite This: J. Phys. Chem. A 2024, 128, 1197−1206

Read Online

. / / 0 1 1 , . / 041, 2530 . 6 0 / 8 2 2 5 9 9 . : A C / 1 5 : 3

**ABSTRACT:** Chiral materials have shown tremendous potential for many technological applications, such as optoelectronics, sensing, magnetism, information technology, and imaging. Characterization of these materials is mostly based on chiroptical spectroscopies, such as electronic circular dichroism (ECD) and circularly polarized luminescence (CPL). These experimental measurements would greatly benefit from theoretical simulations for interpretation of the spectra as well as predictions on new materials. While ECD and CPL simulations are well established for molecular systems, they are not for materials. In this Perspective, we describe the theoretical quantities necessary to simulate ECD and CPL spectra in oriented systems. Then, we discuss the approximate strategies currently used to perform these calculations, what computational machinery is already available to develop more general approaches, and some of the open challenges for the simulation of ECD and CPL spectra in solid materials. When methods that are as reliable and computationally efficient as those for molecules are developed, these simulations will provide invaluable insight and guidance for the rational design of optically active materials.

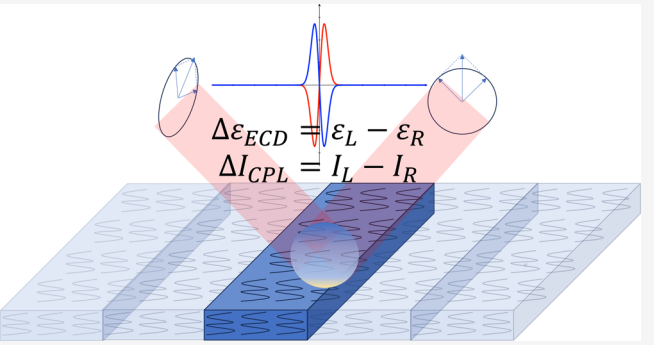


## 1. INTRODUCTION

Molecular and supramolecular chirality have always played an important role in chemistry, as life has developed around building blocks of specific handedness (L-amino acids and D-sugars), a phenomenon known as homochirality. This has enormous implications, for instance, in drug design, as only one enantiomer of a particular compound will have the desired pharmacological effect. However, in recent years supramolecular chirality has shown tremendous potential for other technological applications, like optoelectronics, sensing, magnetism, information technology, and imaging.[1−11] These applications typically require chromophoric groups that can easily absorb and emit light and move energy or charge efficiently. The chirality in the material may be an intrinsic property of the chromophore, like in helicenes,[12−18] or be imprinted by attaching a chiral substituent on an achiral chromophore.[6,8,19] This molecular-scale chirality then influences the aggregation of the constituent units, leading to a chiral supramolecular assembly. However, the supramolecular structure is also influenced by the preparation method, which often leads to polymorphism within the same sample.[6]

Because of the nature of the technological applications of these materials, their characterization often relies on spectroscopic techniques based on their interaction with chiral light, i.e., circularly polarized light. The dominant techniques are electronic circular dichroism (ECD),[6,20−23] which measures the difference in absorption between left and right circularly polarized light, and its emission analogue, circularly polarized luminescence (CPL).[13,16,18,20,24−26] ECD is sensitive to both the intrinsic chiral nature of the chromophoric units and the supramolecular chirality of the assembly. CPL can provide important information about the structural reorganization of the material after absorption and charge transport dynamics. Furthermore, the intrinsic luminescence of the material may be a target property in and on itself, for instance, for the fabrication of circularly polarized-organic light emitting diodes (CP-OLEDs).[17,27,28]

The application of these techniques relies on complementary theoretical simulations, which can help elucidate structure−property relations. However, while simulation of ECD and even CPL spectra are now routine for molecules thanks to robust and easy-to-use implementations of time-dependent density functional theory (TDDFT) and excited state energy gradients (which allow relatively reliable geometry optimizations of the

Received: December 11, 2023
Revised: January 8, 2024
Accepted: January 9, 2024
Published: January 31, 2024

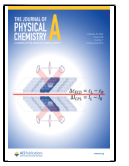







https://doi.org/10.1021/acs.jpca.3c08095
J. Phys. Chem. A 2024, 128, 1197−1206

first excited state),[29−33] this is not the case for extended materials. In fact, most simulations for these materials are based on molecular clusters and excitonic models for the interaction between spatially separated chromophores. However, these approaches rely on significant assumptions, e.g., localized excitations and structural rigidity, that may not always be valid. Therefore, robust methods that are agnostic about the electronic response are desirable, for instance, based on TDDFT with periodic boundary conditions (PBCs), but so far they are not commonly available. In this Perspective, we discuss the theoretical quantities that need to be evaluated to simulate ECD and CPL spectra of oriented solid materials and the current state of the quantum mechanical methods to calculate these quantities. This work does not aim to provide a comprehensive review of the literature but rather to discuss the challenges and the opportunities to develop computational tools for the simulation of ECD and CPL spectra for materials that are as reliable and accessible as for molecules. Such methods would provide invaluable guidance for the interpretation of experimental spectra and may help in the definition of rational design principles for the development of new materials with target chiroptical properties.

The paper is organized as follows. Section 2 describes the theoretical quantities necessary to simulate ECD and CPL spectra in oriented systems. In section 3, we discuss the approximate strategies currently used to perform these calculations, what computational machinery is already available to develop more general approaches, and some of the open challenges for the simulation of ECD and CPL spectra in solid materials. Section 4 provides a summary of the work and concluding remarks.

## 2. THEORY

ECD is defined as the difference in absorption between left and right circularly polarized light for electronic transitions (generally expressed in terms of the molar extinction coefficient) whereas CPL is the corresponding difference in emission (generally expressed in terms of intensity):[20]

$$\Delta\varepsilon_{\mathrm{ECD}} = \varepsilon_{\mathrm{L}} - \varepsilon_{\mathrm{R}}$$
$$\Delta I_{\mathrm{CPL}} = I_{\mathrm{L}} - I_{\mathrm{R}} \tag{1}$$

Dissymmetry factors express the same quantities relative to the total absorption and emission:

$$g_{\mathrm{abs}} = \frac{\varepsilon_{\mathrm{L}} - \varepsilon_{\mathrm{R}}}{\varepsilon} = \frac{\varepsilon_{\mathrm{L}} - \varepsilon_{\mathrm{R}}}{\frac{1}{2}(\varepsilon_{\mathrm{L}} + \varepsilon_{\mathrm{R}})}$$
$$g_{\mathrm{lum}} = \frac{I_{\mathrm{L}} - I_{\mathrm{R}}}{I} = \frac{I_{\mathrm{L}} - I_{\mathrm{R}}}{\frac{1}{2}(I_{\mathrm{L}} + I_{\mathrm{R}})} \tag{2}$$

Despite the difference in name, ECD and CPL describe the same phenomenon in absorption and in emission, respectively. Therefore, the key quantity for the simulation of both types of spectra in oriented systems is the same, i.e., the rotatory strength tensor:[31,34]

$$R^{\mathrm{if}}_{\alpha\beta} = \frac{1}{2}(\mathrm{Im}\{\mu^{\mathrm{if}}_{\alpha} m^{\mathrm{if}*}_{\beta}\} + \mathrm{Im}\{\mu^{\mathrm{if}}_{\beta} m^{\mathrm{if}*}_{\alpha}\} + \frac{1}{3}\omega_{\mathrm{if}}\,\mathrm{Re}\{\varepsilon_{\alpha\gamma\delta}\mu^{\mathrm{if}}_{\gamma}\Theta^{\mathrm{if}*}_{\delta\beta} + \varepsilon_{\beta\gamma\delta}\mu^{\mathrm{if}}_{\gamma}\Theta^{\mathrm{if}*}_{\delta\alpha}\}) \tag{3}$$

where i/f represent the initial and final electronic states with transition frequency $\omega_{\mathrm{if}}$ and Greek letters refer to Cartesian coordinates (repeated indexes imply a summation over all values). For ECD, i is the ground state and f is an excited state, while for CPL i is typically the first excited state (because of Kasha's rule) and f is the ground state. However, given the symmetry of the tensors, the CPL rotatory strength is the same as that for the ECD from the ground to the first excited state at the optimized geometry of the first excited state. The transition moment between the initial and final states for the electric dipole is $\mu^{\mathrm{if}}_{\alpha} = \langle \mathrm{i}|\hat{\mu}_{\alpha}|\mathrm{f}\rangle$, and similarly for the magnetic dipole $m^{\mathrm{if}}_{\alpha}$ and the electric quadrupole $\Theta^{\mathrm{if}}_{\delta\alpha}$. For a beam along a given direction $\mathbf{n}$, the quantity corresponding to the measured observable is[31]

$$R^{\mathrm{if}}_{\mathbf{n}} = \mathbf{n}^{\dagger}\tilde{\mathbf{R}}^{\mathrm{if}}\mathbf{n} \tag{4}$$

where the tensor $\tilde{\mathbf{R}}^{\mathrm{if}}$ is

$$\tilde{R}^{\mathrm{if}}_{\alpha\beta} = \frac{1}{2}[\mathrm{Tr}(\mathbf{R}^{\mathrm{if}})\delta_{\alpha\beta} - R^{\mathrm{if}}_{\alpha\beta}] \tag{5}$$

The rotatory strength expressions in eqs 3−5 are more complicated than those for isotropic samples, which only involve the terms with the transition magnetic dipole (the first line in eq 3). This is because in isotropic samples the measured quantity is the spatial average of all possible orientations: $R^{\mathrm{if}} = \mathrm{Tr}(\mathbf{R}^{\mathrm{if}})/3$, and the terms with the quadrupole transition moment do not contribute to this trace. However, for oriented systems like crystals and thin films, one needs the full tensor defined above.

Since most calculations are performed with a static picture, i.e., computing $\mathbf{R}^{\mathrm{if}}$ from an optimized geometry possibly for multiple final states, one can only obtain a stick spectrum. Broadening is typically included with a Gaussian envelope, such that the intensities (in cgs units of $10^{-40}$ esu$^2$ cm$^2$) are

$$\Delta\varepsilon(\omega) = \frac{\omega_{\mathrm{if}} R^{\mathrm{if}}_{\mathbf{n}}}{2.296 \times 10^{-39}\sqrt{\pi}\sigma} \mathrm{e}^{-((\omega-\omega_{0\mathrm{f}})/\sigma)^2} \tag{6}$$

where $\omega_{\mathrm{if}}$ is the transition frequency and $\sigma$ is the broadening parameter that are expressed in the same units and $R^{\mathrm{if}}_{\mathbf{n}}$ is expressed in cgs units of $10^{-40}$ erg esu cm G$^{-1}$. A vibrational progression can be included explicitly with techniques similar to those used for molecules.[35,36]

The review above shows that simulations of ECD and CPL require the evaluation of transition energies and moments for extended systems. Currently, the most general formulation employs PBCs. However, the electric and magnetic dipole operators do not have the correct translational symmetry. An approximate form of the electronic electric dipole operator ($\boldsymbol{\mu} = -e\mathbf{r}$) that satisfies PBCs has been introduced a few decades ago to compute electric dipole polarizability tensors:[37,38]

$$\mathbf{r} \simeq \mathrm{i}\mathrm{e}^{\mathrm{i}\mathbf{k}\cdot\mathbf{r}}\nabla_{k}\mathrm{e}^{-\mathrm{i}\mathbf{k}\cdot\mathbf{r}} \tag{7}$$

where $\mathbf{k}$ is the wave vector in reciprocal space. More recently, an equivalent form of the magnetic dipole and electric quadrupole moments have been proposed in the context of optical rotation:[39−41]

$$\hat{\underline{\mathbf{m}}} = \underline{C}^{\dagger}\tilde{\underline{\mathbf{m}}}\underline{C} - \frac{\mathrm{i}}{2}\underline{C}^{\dagger}\underline{\mathbf{p}}\underline{C} \times \underline{\mathbf{U}} \tag{8}$$

$$\hat{\underline{\boldsymbol{\Theta}}} = \underline{C}^{\dagger}\tilde{\underline{\boldsymbol{\Theta}}}\underline{C} + \mathrm{i}\underline{C}^{\dagger}\underline{\mathbf{p}}\underline{C} \odot \underline{\mathbf{U}} \tag{9}$$

where the underbar indicates quantities expressed in the crystalline orbital (CO) basis with coefficients $\underline{C}$, the tilde indicates symmetrization with respect to forward and backward replication of the unit cell along the translation vectors, $\mathbf{p}$ is the


https://doi.org/10.1021/acs.jpca.3c08095
J. Phys. Chem. A 2024, 128, 1197−1206

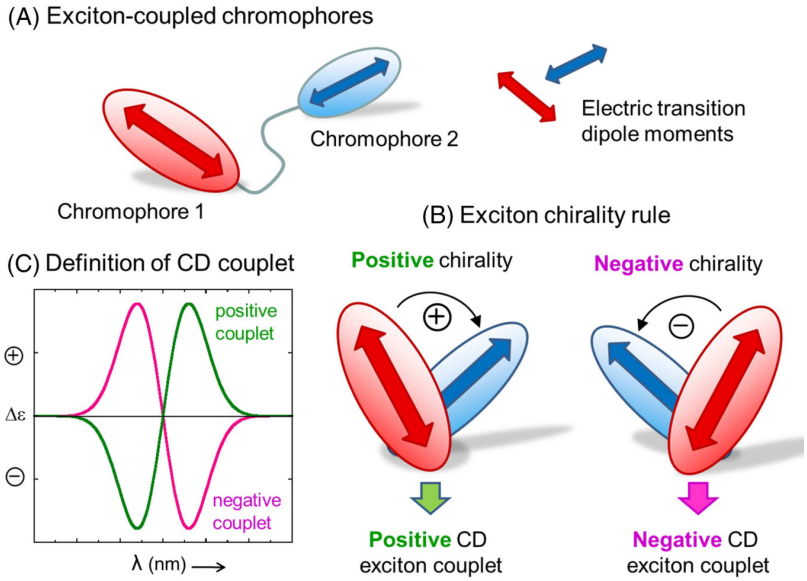


**Figure 1.** Schematic representation of the exciton chirality method (ECM) for the simulation of ECD. (A) Exciton-coupled chromophores and their transition dipole moments. (B) Definition of the CD exciton couplet and its sign. (C) Formulation of the exciton chirality rule. Reprinted with permission from ref 49. Copyright 2021 The Author.

momentum operator, and $\underline{\mathbf{U}}$ is the vector of matrices that transforms the CO coefficients $\underline{C}$ to their gradient with respect to $\mathbf{k}$, $\nabla_{\mathbf{k}}\underline{C} = \underline{C}\underline{\mathbf{U}}$.[37] Although formulated for the OR, these expressions can be used to compute the transition moments between electronic states as shown in eq 3.

Alternatively, since molar rotation $[\alpha]_\omega$ and molar ellipticity $[\theta]_\omega$ (the latter is directly proportional to $\Delta\varepsilon$) are related by Kramers−Kronig (KK) transformations:[42−44]

$$[\alpha]_\omega = \frac{2\omega^2}{\pi}\int_0^\infty \frac{[\theta]_\xi}{\xi(\xi^2-\omega^2)}\,\mathrm{d}\xi$$
$$[\theta]_\omega = -\frac{2\omega^3}{\pi}\int_0^\infty \frac{[\alpha]_\xi}{\xi^2(\xi^2-\omega^2)}\,\mathrm{d}\xi \qquad (10)$$

one could also obtain the ECD spectrum in a certain frequency region from the OR dispersion (ORD) curve in the same region, and vice versa. This approach requires that a phenomenological lifetime is included in the linear response function to avoid unphysically large values of the property around its poles, which makes the response function complex, even in real space.

A final note is that the discussion above concerns the simulation of true ECD and CPL signals in chiral extended materials. However, experimental measurements are plagued by interference from macroscopic anisotropies in the solid state, i.e., linear dichroism (LD) and linear birefringence (LB); see for instance ref 6. for a more detailed discussion. One interference effect appears when the main axes of LD and LB do not align; this is a real effect in the sense that it is not due to the instrument. Other effects are instrumental artifacts that can be due to the polarization modulation technique or the photomultiplier. Experimentalists have devised various solutions to isolate or eliminate these interference effects,[6,10,25,45−48] but these are beyond the scope of this work. Also in this case, simulations would provide important validation for these techniques.

## 3. METHODS

In this section, we discuss methods that are currently available to simulate ECD and CPL spectra as well as methods that provide some of the pieces of information necessary to evaluate the spectra. The former are obviously more approximate methods, which can be applied under opportune conditions, while the latter are more general approaches that can be extended to cover ECD and CPL.

Most of the calculations of ECD and CPL in materials have been done using the exciton chirality method (ECM), which is based on the exciton coupling between coupled oscillators; see Figure 1.[12,49−54] This method can be used when a chiral molecule contains two or more "separate" chromophores undergoing electric-dipole-allowed transitions; in a molecular material, the coupled transitions can occur between separate molecular units. If the relative orientation of the chromophores and the orientation of the electric transition dipole for each chromophore are known, then the ECM provides a fairly simple way to determine the ECD spectrum of the system. This method still relies on quantum mechanical (QM) calculations to evaluate the transition dipoles (or the 3D transition density in more elaborate formulations) for the transitions on individual chromophores.[49] However, the QM calculations are limited to individual molecules (or molecular fragments), bypassing the burden of treating the extended system as a whole. The first limitation of the ECM is that it requires knowledge of the relative orientation of the chromophores. In part, this is a general issue for chiral materials, e.g., when multiple polymorphs are present in the sample or when large floppy chromophores are used,[6] as discussed more in detail later on. However, it is particularly taxing for the ECM based on molecular calculations because the latter cannot easily recover the packing in a material (using, for instance, standard geometry optimizations) unless it is known by other means (e.g., experiment) or the molecular units are rigid (e.g., helicenes). A more important issue is whether the overall spectrum is dominated by the excitonic process, while other processes, like the intrinsic chirality of the chromophore or electron delocalization, can be neglected. This is hard to assess beforehand, which limits the predictive power of the ECM. Therefore, a direct evaluation of the spectra from a


https://doi.org/10.1021/acs.jpca.3c08095
J. Phys. Chem. A 2024, 128, 1197−1206

QM calculation on the fully extended system would be preferable.

An intermediate step between exciton models and full QM calculations is represented by tight-binding models.[55] Tight-binding models build an *ad hoc* Hamiltonian that only contains interactions between nearest neighbors. Exciton and tight-binding models were also combined to allow calculations when computational resources were still limited.[56,57] These models are very computationally efficient, but they are system-specific and require reference data for the parametrization of the Hamiltonian. Furthermore, longer-range interactions may be important when excited state properties are involved, especially with sensitive properties such as optical activity. Another approach is to neglect the response of the ground state electron density to the external field;[58] this corresponds to approximating excited states as single Slater determinants built from the COs, so that the excitation energies are just orbital energy differences and the transition moments are computed between individual Slater determinants. Although this strategy is also computationally efficient because it sidesteps the linear response calculation, it is not typically a good approximation to obtain excited state energies from differences in orbital energies (otherwise, TDDFT would not be so popular). From this author's experience with OR, the orbital response accounts for about half of the property magnitude; considering the relationship between OR and CD (see eq 10), it seems unlikely that this approach can provide reliable results in general.

The most inclusive route for the simulation of ECD spectra is the extension of molecular linear response methods to solids with PBCs. Given the size of the typical chromophores involved, the best balance between cost and accuracy would most likely be obtained with TDDFT. Although this author is not aware of an implementation of these methods for ECD in general-purpose codes, many pieces are already available, and the time is mature for such developments. A TDDFT-PBC implementation for 1D periodic systems was proposed by Hirata and co-workers in a standalone program, but the focus was only on excitation energies and the method has not been generalized to 3D periodicity.[59] In more recent years, more general implementations of TDDFT have appeared, at least for standard UV/vis absorption.[32,60−70]

However, these implementations often rely on the Tamm−Dancoff approximation (TDA),[66] which is more efficient but less reliable,[71] and are limited to the Γ point in reciprocal space,[67] which simplifies the equations as the CO coefficients are real but at the expense of accuracy. The choice of functional is also not as simple as that for molecules. Optical activity and excited state calculations typically require range-separated hybrid functionals because they better describe the long-range density response. However, the treatment of exact exchange is still problematic for PBC codes. Common approaches include the use of pure functionals (without exact exchange), hybrid functionals with exchange only in the short-range (like HSE06[70,72]), or approximate procedures to include exchange (e.g., the auxiliary density matrix method, ADMM[66,67]). Another issue is the size of the basis set involved. In molecular calculations, large Gaussian-based basis sets with diffuse functions are often recommended for accurate results,[33,73] but these basis sets are problematic for PBC calculations because of linear dependence issues between replicated cells. For bulk conducting materials, plane wave basis sets are used as they naturally satisfy translational symmetry, but for semiconductors or molecular crystals, a large number of these functions are necessary for convergence of energy and properties. Therefore, mixed Gaussian/plane wave basis sets can be used,[65] but they have the same linear-dependence issues mentioned above. Thus, although all of these approaches make PBC calculations feasible, it is unclear whether the accuracy will be sufficient for the ECD and CPL spectra. For instance, a potential issue is that the ECD signal is much smaller (by 2 or 3 orders of magnitude) compared to regular absorption, and each band is often the convolution of multiple signals with opposite sign. Therefore, relatively small errors on individual transitions could lead to qualitatively incorrect spectra. Nonetheless, these limitations may be overcome with a further developmental effort.

Another approach to compute excitation energies in extended systems using linear-response DFT is as poles of the imaginary part of the dielectric function (equivalent to the poles of the electric dipole-electric dipole polarizability tensor).[74] More recently, this approach was extended to include band intensities.[75] Equivalently, one can solve the Bethe−Salpeter equation on top of the GW approximation to evaluate the dielectric function.[61,76,77] In this case, excitation energies are obtained indirectly by scanning a frequency region to find the poles of the polarizability tensor. To obtain the ECD spectrum, one would need the appropriate combination of the polarizabilities for optical activity (electric dipole-magnetic dipole and electric dipole-magnetic quadrupole). Similarly, the ECD spectrum could be obtained from the ORD curve via a KK transformation (see eq 10), which is obtained from the real part of the same optical activity tensors. However, the OR tensor for PBC methods would need to be extended to accommodate a lifetime parameter. An example of both approaches for a molecular case is reported in Figure 2. Finding the poles of a response function by scanning a frequency range rather than calculating the excitation energies directly would circumvent the need for a TDDFT-PBC implementation, but its applicability seems cumbersome. In fact, one would need to repeat the OR calculation at many frequencies, with tighter grids around the poles' regions, to obtain a reasonable discretization of the dielectric function or of the KK integrals.

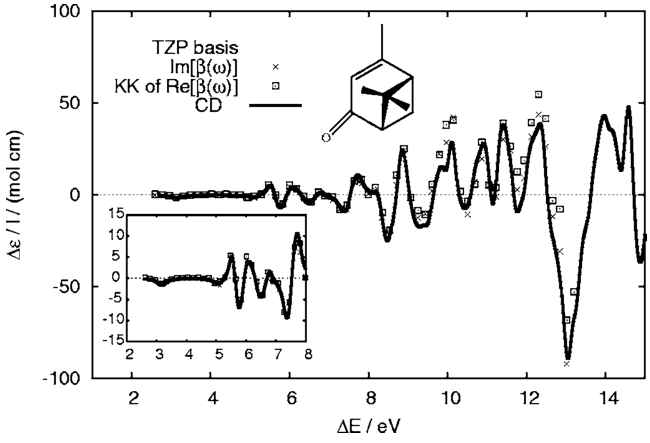


**Figure 2.** ECD spectrum of (1*S*,5*S*)-verbenone from the rotatory strengths (solid line, antisymmetrized Lorentz broadening), from $\mathrm{Im}(\tilde{\beta})$ (crosses), converted to $\delta\varepsilon$ and from $\mathrm{Re}(\tilde{\beta})$ (squares), and converted to $\delta\varepsilon$ after the KK transformation. Inset: CD spectrum from $\mathrm{Im}(\tilde{\beta})$ and $\mathrm{Re}(\tilde{\beta})$. In this notation, the real and imaginary parts of the optical rotation parameter $\tilde{\beta}$ are proportional to the molar rotation and the molar ellipticity, respectively; see eq 10. Reprinted with permission from ref 44. Copyright 2006 AIP Publishing.



https://doi.org/10.1021/acs.jpca.3c08095
J. Phys. Chem. A 2024, 128, 1197−1206

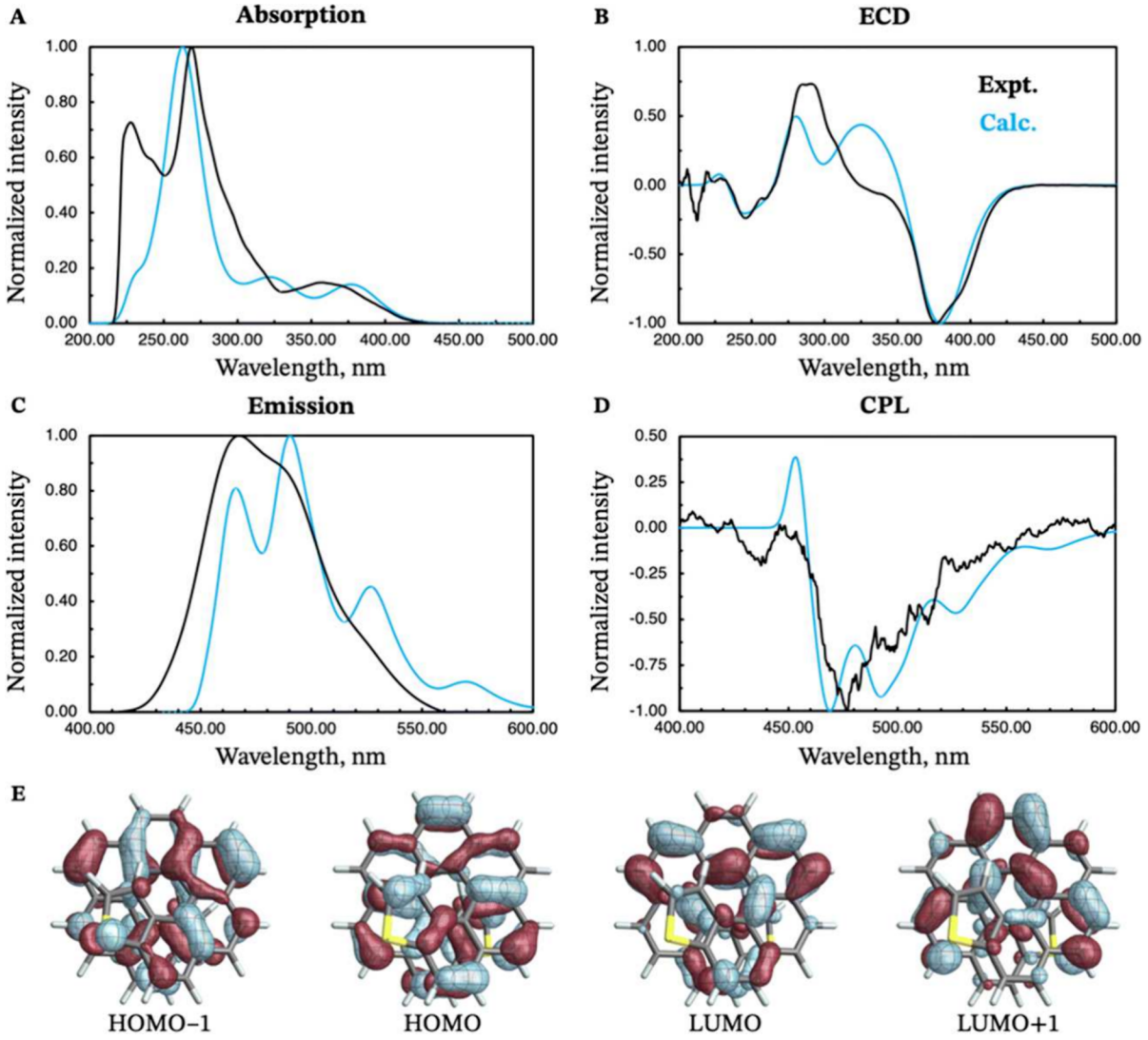


**Figure 3.** Experimental (black curves) and calculated (blue curves) absorption (panel A), ECD (panel B), emission (panel C), and CPL (panel D) spectra of (M)-exodithia[9]helicene. Isosurfaces (±0.03 au) for the most relevant frontier molecular orbitals (HOMO−1, HOMO, LUMO, and LUMO+1) are shown in panel E. The calculated energies were shifted by −0.40 eV prior to conversion to wavelengths. Reprinted with permission from ref 16. Copyright 2022 Royal Society of Chemistry.

The simulation of CPL spectra introduces another challenge beyond those discussed so far: the transition occurs from the minimum structure in the first excited state. Excited state geometry optimizations are rather uncommon with PBC methods, although some examples have appeared.[66] Current simulations of CPL spectra in extended systems rely on geometry optimization of individual molecular units within the material. This works as long as the chromophore is fairly rigid, and again helicenes are a good example;[12−18] see the example in Figure 3. However, many new materials are based on conjugated polymers or floppy chromophores, where the nature of the excited state electron density distribution may be different from that of the ground state. In these cases, the geometry from where the emission occurs may be significantly influenced by packing of the solid state environment around the chromophore. Thus, geometry optimization of the excited state geometry of the extended system would be required for reliable simulations.

An important issue that goes beyond the development of appropriate electronic structure methods is the conformational search and polymorphism. Because of the nature of the systems involved in thin films and electronic materials, considering a single geometric configuration may not be sufficient. In fact, in many cases the material's structure is unknown and the effective signal is the sum of contributions form multiple polymorphs.[6] Therefore, strategies for conformational searches will be necessary, and spectra will be calculated for multiple configurations. These searches could be performed with classical molecular dynamics (MD) simulations or with other available protocols.[51,78,79] Then, the relevant structures would be optimized at the QM level in the ground state for ECD and possibly in the first excited state for CPL. In the excited state, one may find multiple minimum structures that could be accessible from these ground state conformers. However, in principle, one would also need to consider the dynamics in the excited states directly, where multiple minima in the first excited state could be reached from a vertical excitation to a higher excited state from a particular ground state geometry. These other first excited state minima cannot be found with a direct geometry optimization from the ground state geometry. Instead, one would need to perform an MD simulation directly in the


https://doi.org/10.1021/acs.jpca.3c08095
J. Phys. Chem. A 2024, 128, 1197−1206

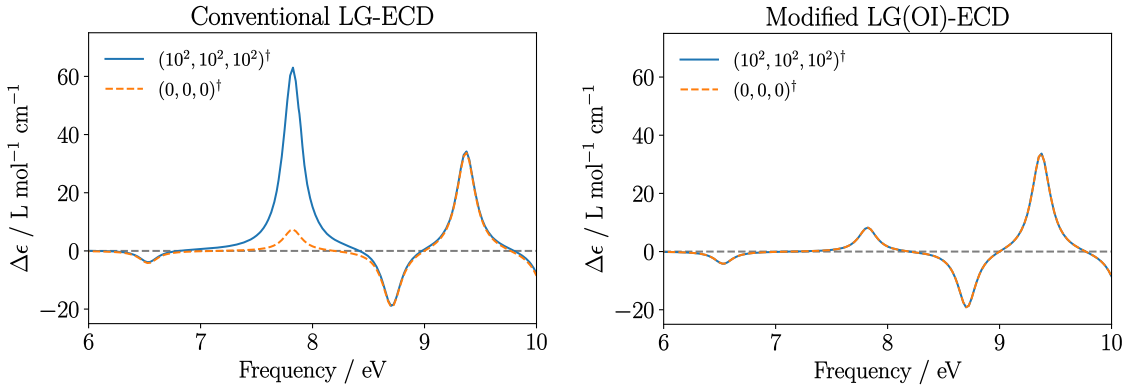


**Figure 4.** Comparison of the conventional and modified LG-ECD as a function of the frequency for the hydrogen peroxide molecule. For each method, the ECD is shown with the gauge origin placed in either the center of mass of the molecule $[(0, 0, 0)^T]$ or translated to $(10^2, 10^2, 10^2)^T$ Å. Reprinted with permission from ref 83. Copyright 2022 The Authors.

excited state. Perhaps, one could use excited state charges from a TDDFT calculation to perform a classical MD simulation in the first excited state (similar to what is done for excited state molecules in solution). Although not necessarily accurate, this procedure may lead to multiple conformations in the first excited state that could be refined with QM geometry optimization. This protocol will obviously increase the overall computational cost, as the DFT calculations will be repeated on multiple structures. However, the number of relevant configurations will be significantly smaller than those necessary when dealing with solution phase simulations.

An issue that is characteristic of chiroptical simulations is the choice of gauge for the representation of the dipole (and quadrupole) operator. The representation in terms of the position operator is called the length gauge (LG). This is the natural choice for standard absorption simulations to calculate the oscillator strength. However, since the electric dipole interacts with the magnetic dipole (and electric quadrupole) in the rotatory strength, the length gauge formulation leads to values that are origin dependent. In OR calculations, this is commonly solved by using basis functions that are explicitly dependent on the magnetic field, known as London orbitals or gauge including atomic orbitals (GIAOs).[80] These can be used for transition properties as well, but they lead to cumbersome expressions.[31] Therefore, most programs report the rotatory strength in the velocity gauge (VG), where the electric dipole is represented by the momentum operator. The two choices of gauge are numerically equivalent only for exact methods or in the complete basis set limit for variational methods like DFT (although we showed that gauge invariance with approximate functionals does not imply accuracy, as different functionals converge to different results[73]). Recently, we have proposed a strategy to overcome the origin-dependence issue of the LG rotatory strength without using GIAOs; a method we called origin-invariant LG or LG(OI);[81−83] see Figure 4. Both the VG and LG(OI) approaches were implemented for the OR calculations with DFT-PBC[40] and can be easily extended to TDDFT-PBC simulations of ECD and CPL spectra.

Although there is a growing interest in supramolecular organic materials with chiroptical properties, the most luminescent systems include heavy elements, especially lanthanides.[27,84−86] Emission often occurs between states of different spin due to strong spin−orbit coupling. Therefore, calculations must include relativistic effects to simulate the CPL spectra. A number of studies have been published that include such effects for molecules; see for instance the plots in Figure 5, which report circularly polarized phosphorescence (CPP, i.e., CPL from the lowest triplet state to the ground singlet state) for an organic molecule including vibrational effects at the Franck−Condon (FC) and Herzberg−Teller (FCHT) levels.[18,35,86,87] These approaches need to be extended to periodic calculations.

A more accurate description of the ECD spectrum should include vibronic effects. These contributions can come from modes localized on a single molecular unit within the extended system, through interactions between neighbors, or as collective effects of the extended system. The first effect can be treated with techniques used for molecules; see again Figure 5.[35,36] Models for interactions between molecular units have also been developed within an excitonic picture.[88] The last type of interaction, exciton−phonon coupling, is harder to describe, and it requires a vibrational calculation including PBCs.

## 4. CONCLUSIONS

In this Perspective, we discuss how to perform simulations of ECD and CPL spectra for chiral oriented systems in the solid phase. These materials have attracted increasing attention for a variety of technological applications, including optoelectronics, sensing, magnetism, information technology, and imaging. Experimentally, the characterization of the materials virtually always includes ECD spectroscopy, while strong CPL is often a sought-after property for applications in devices. Theoretical simulations that can help interpret the experimental spectra or predict structures with specific chiroptical properties are extremely desirable. However, so far, these simulations are based on molecular calculations on individual chromophoric systems or on exciton coupling models between two or more isolated chromophoric units. These models are powerful, but they rely on stringent assumptions that are not always valid (e.g., they do not work when electron conjugation extends across chromophores).

Thus, more general approaches are desirable that make no assumptions about the intrinsic electronic structure of the system. Given the size of the chromophores involved in real applications, the most promising approach is based on TDDFT-PBC methods combined with fast and reliable conformational search algorithms. In this work, we outline the required quantities to be calculated and the corresponding challenges. Much progress has been done in the past 10−20 years for these types of methods, and most pieces are now available that can be extended and properly combined for the simulation of ECD and


https://doi.org/10.1021/acs.jpca.3c08095
J. Phys. Chem. A 2024, 128, 1197−1206

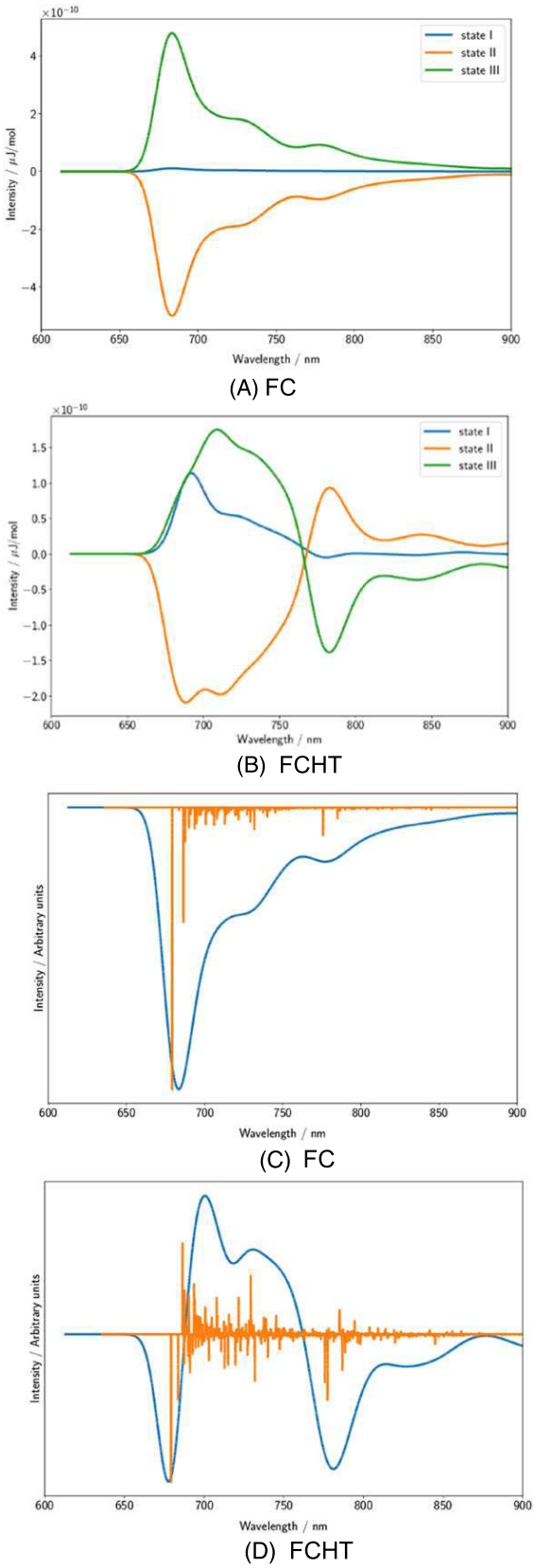


**Figure 5.** Calculated FC and FCHT CPP sum spectra of (1R)-camphorquinone. The spectra in panels (A) and (B) show the contribution due to each triplet state; panels (C) and (D) show the sum spectra. Intensities were in arbitrary units. Reprinted with permission from ref 35. Copyright 2018 John Wiley and Sons.

CPL spectra. Once software is developed that is sufficiently robust and efficient, simulations will provide invaluable insight and guidance for the rational design of optically active materials.

## AUTHOR INFORMATION


### Corresponding Author

**Marco Caricato** − *Department of Chemistry, University of Kansas, Lawrence, Kansas 66045, United States;* orcid.org/0000-0001-7830-0562; Email: mcaricato@ku.edu

Complete contact information is available at: https://pubs.acs.org/10.1021/acs.jpca.3c08095


### Notes

The author declares no competing financial interest.

### Biography

Marco Caricato earned his M.S. in Chemistry at the Università di Pisa (Italy) in 2003 and his Ph.D. in Chemistry at the Scuola Normale Superiore (Italy) in 2006 under the supervision of Jacopo Tomasi. From 2006 to 2010, he worked as postdoctoral researcher with Ken Wiberg at Yale University, and from 2010 to 2014 as research scientist at Gaussian, Inc. before becoming a professor at the University of Kansas in 2014. His research interests involve the development and application of quantum mechanical methods to condensed phase systems for the investigation of reactivity, catalysis, and light−matter interactions.

## ACKNOWLEDGMENTS

The author gratefully acknowledges support from the National Science Foundation through Grant No. CHE-2154452. The author would also like to thank Prof. Lorenzo di Bari for useful discussions.

## REFERENCES


(1) Rong, R.; Liu, Y.; Nie, X.; Zhang, W.; Zhang, Z.; Liu, Y.; Guo, W. The Interaction of 2D Materials With Circularly Polarized Light. *Adv. Sci.* **2023**, *10*, 2206191.

(2) Takaishi, K.; Maeda, C.; Ema, T. Circularly polarized luminescence in molecular recognition systems: Recent achievements. *Chirality* **2023**, *35*, 92−103.

(3) García, F.; Gómez, R.; Sánchez, L. Chiral supramolecular polymers. *Chem. Soc. Rev.* **2023**, *52*, 7524−7548.

(4) Khasbaatar, A.; Xu, Z.; Lee, J.-H.; Campillo-Alvarado, G.; Hwang, C.; Onusaitis, B. N.; Diao, Y. From Solution to Thin Film: Molecular Assembly of π-Conjugated Systems and Impact on (Opto)electronic Properties. *Chem. Rev.* **2023**, *123*, 8395−8487.

(5) Song, I.; Ahn, J.; Ahn, H.; Lee, S. H.; Mei, J.; Kotov, N. A.; Oh, J. H. Helical polymers for dissymmetric circularly polarized light imaging. *Nature* **2023**, *617*, 92−99.
(6) Albano, G.; Pescitelli, G.; Di Bari, L. Chiroptical Properties in Thin Films of π-Conjugated Systems. *Chem. Rev.* **2020**, *120*, 10145−10243.
(7) Zinna, F.; Albano, G.; Taddeucci, A.; Colli, T.; Aronica, L. A.; Pescitelli, G.; Di Bari, L. Emergent Nonreciprocal Circularly Polarized Emission from an Organic Thin Film. *Adv. Mater.* **2020**, *32*, 2002575.
(8) Albano, G.; Gorecki, M.; Pescitelli, G.; Di Bari, L.; Javorfi, T.; Hussain, R.; Siligardi, G. Electronic circular dichroism imaging (CD i) maps local aggregation modes in thin films of chiral oligothiophenes. *New J. Chem.* **2019**, *43*, 14584−14593.
(9) Zinna, F.; Resta, C.; Górecki, M.; Pescitelli, G.; Di Bari, L.; Jávorfi, T.; Hussain, R.; Siligardi, G. Circular Dichroism Imaging: Mapping the Local Supramolecular Order in Thin Films of Chiral Functional Polymers. *Macromol.* **2017**, *50*, 2054−2060.
(10) Albano, G.; Pescitelli, G.; Di Bari, L. Reciprocal and Non-reciprocal Chiroptical Features in Thin Films of Organic Dyes. *ChemNanoMat* **2022**, *8*, No. e202200219.
(11) Shen, C.; Srebro-Hooper, M.; Weymuth, T.; Krausbeck, F.; Navarrete, J. T. L.; Ramirez, F. J.; Nieto-Ortega, B.; Casado, J.; Reiher, M.; Autschbach, J.; Crassous, J.; et al. Redox-Active Chiroptical Switching in Mono- and Bis-Iron Ethynylcarbo[6]helicenes Studied by Electronic and Vibrational Circular Dichroism and Resonance Raman Optical Activity. *Chem.—Eur. J.* **2018**, *24*, 15067−15079.
(12) You, L.; Pescitelli, G.; Anslyn, E. V.; Di Bari, L. An Exciton-Coupled Circular Dichroism Protocol for the Determination of Identity, Chirality, and Enantiomeric Excess of Chiral Secondary Alcohols. *J. Am. Chem. Soc.* **2012**, *134*, 7117−7125.
(13) Abbate, S.; Longhi, G.; Lebon, F.; Castiglioni, E.; Superchi, S.; Pisani, L.; Fontana, F.; Torricelli, F.; Caronna, T.; Villani, C.; et al. Helical Sense-Responsive and Substituent-Sensitive Features in Vibrational and Electronic Circular Dichroism, in Circularly Polarized Luminescence, and in Raman Spectra of Some Simple Optically Active Hexahelicenes. *J. Phys. Chem. C* **2014**, *118*, 1682−1695.
(14) Duwald, R.; Bosson, J.; Pascal, S.; Grass, S.; Zinna, F.; Besnard, C.; Di Bari, L.; Jacquemin, D.; Lacour, J. Merging polyacenes and cationic helicenes: from weak to intense chiroptical properties in the far red region. *Chem. Sci.* **2020**, *11*, 1165−1169.
(15) Cei, M.; Di Bari, L.; Zinna, F. Circularly polarized luminescence of helicenes: A data-informed insight. *Chirality* **2023**, *35*, 192−210.
(16) Baciu, B. C.; Bronk, P. J.; de Ara, T.; Rodriguez, R.; Morgante, P.; Vanthuyne, N.; Sabater, C.; Untiedt, C.; Autschbach, J.; Crassous, J.; Guijarro, A.; et al. Dithia[9]helicenes: Molecular design, surface imaging, and circularly polarized luminescence with enhanced dissymmetry factors. *J. Mater. Chem. C* **2022**, *10*, 14306−14318.
(17) Dhbaibi, K.; Abella, L.; Meunier-Della-Gatta, S.; Roisnel, T.; Vanthuyne, N.; Jamoussi, B.; Pieters, G.; Racine, B.; Quesnel, E.; Autschbach, J.; et al. Achieving high circularly polarized luminescence with push−pull helicenic systems: from rationalized design to top-emission CP-OLED applications. *Chem. Sci.* **2021**, *12*, 5522−5533.
(18) Dhbaibi, K.; Morgante, P.; Vanthuyne, N.; Autschbach, J.; Favereau, L.; Crassous, J. Low-Temperature Luminescence in Organic Helicenes: Singlet versus Triplet State Circularly Polarized Emission. *J. Phys. Chem. Lett.* **2023**, *14*, 1073−1081.
(19) Albano, G.; Aronica, L. A.; Minotto, A.; Cacialli, F.; Di Bari, L. Chiral Oligothiophenes with Remarkable Circularly Polarized Luminescence and Electroluminescence in Thin Films. *Chem.—Eur. J.* **2020**, *26*, 16622−16627.
(20) Barron, L. D. *Molecular Light Scattering and Optical Activity*; Cambridge University Press: Cambridge, UK; New York, 2004.
(21) Pescitelli, G.; Di Bari, L.; Berova, N. Application of electronic circular dichroism in the study of supramolecular systems. *Chem. Soc. Rev.* **2014**, *43*, 5211−5233.
(22) Górecki, M.; Lipparini, F.; Albano, G.; Jávorfi, T.; Hussain, R.; Siligardi, G.; Pescitelli, G.; Di Bari, L. Electronic Circular Dichroism Imaging (ECDi) Casts a New Light on the Origin of Solid-State Chiroptical Properties. *Chem.—Eur. J.* **2022**, *28*, No. e202103632.
(23) Taddeucci, A.; Zinna, F.; Siligardi, G.; Di Bari, L. Circularly Polarized Microscopy of Thin Films of Chiral Organic Dyes. *Chem. Biomed. Imaging* **2023**, *1*, 471−478.
(24) Albano, G.; Taddeucci, A.; Pescitelli, G.; Di Bari, L. Spatially Resolved Chiroptical Spectroscopies Emphasizing Recent Applications to Thin Films of Chiral Organic Dyes. *Chem.—Eur. J.* **2023**, *29*, No. e202301982.
(25) Longhi, G.; Castiglioni, E.; Koshoubu, J.; Mazzeo, G.; Abbate, S. Circularly Polarized Luminescence: A Review of Experimental and Theoretical Aspects. *Chirality* **2016**, *28*, 696−707.
(26) Dhbaibi, K.; Favereau, L.; Srebro-Hooper, M.; Quinton, C.; Vanthuyne, N.; Arrico, L.; Roisnel, T.; Jamoussi, B.; Poriel, C.; Cabanetos, C.; et al. Modulation of circularly polarized luminescence through excited-state symmetry breaking and interbranched exciton coupling in helical push−pull organic systems. *Chem. Sci.* **2020**, *11*, 567−576.
(27) Zinna, F.; Pasini, M.; Galeotti, F.; Botta, C.; Di Bari, L.; Giovanella, U. Design of Lanthanide-Based OLEDs with Remarkable Circularly Polarized Electroluminescence. *Adv. Funct. Mater.* **2017**, *27*, 1603719.
(28) Arrico, L.; Di Bari, L.; Zinna, F. Quantifying the Overall Efficiency of Circularly Polarized Emitters. *Chem.—Eur. J.* **2021**, *27*, 2920−2934.
(29) Srebro-Hooper, M.; Autschbach, J. Calculating Natural Optical Activity of Molecules from First Principles. *Annu. Rev. Phys. Chem.* **2017**, *68*, 399−420.
(30) Rudolph, M.; Autschbach, J. Performance of Conventional and Range-Separated Hybrid Density Functionals in Calculations of Electronic Circular Dichroism Spectra of Transition Metal Complexes. *J. Phys. Chem. A* **2011**, *115*, 14677−14686.
(31) Autschbach, J. Time-Dependent Density Functional Theory for Calculating Origin-Independent Optical Rotation and Rotatory Strength Tensors. *ChemPhysChem* **2011**, *12*, 3224−3235.
(32) Casida, M. E. Time-dependent density-functional theory for molecules and molecular solids. *J. Mol. Struct.: THEOCHEM* **2009**, *914*, 3−18.
(33) Srebro, M.; Govind, N.; de Jong, W. A.; Autschbach, J. Optical rotation calculated with time-dependent density functional theory: the OR45 benchmark. *J. Phys. Chem. A* **2011**, *115*, 10930−10949.
(34) Pedersen, T. B.; Hansen, A. E. Ab initio calculation and display of the rotary strength tensor in the random phase approximation. Method and model studies. *Chem. Phys. Lett.* **1995**, *246*, 1−8.
(35) Egidi, F.; Fusè, M.; Baiardi, A.; Bloino, J.; Li, X.; Barone, V. Computational simulation of vibrationally resolved spectra for spin-forbidden transitions. *Chirality* **2018**, *30*, 850−865.
(36) Pritchard, B.; Autschbach, J. Calculation of the Vibrationally Resolved, Circularly Polarized Luminescence of d-Camphorquinone and (S,S)-trans-β-Hydrindanone. *ChemPhysChem* **2010**, *11*, 2409−2415.
(37) Kudin, K. N.; Scuseria, G. E.; Scuseria, G. E. An efficient finite field approach for calculating static electric polarizabilities of periodic systems. *J. Chem. Phys.* **2000**, *113*, 7779.
(38) Izmaylov, A. F.; Brothers, E. N.; Scuseria, G. E. Linear-scaling calculation of static and dynamic polarizabilities in Hartree-Fock and density functional theory for periodic systems. *J. Chem. Phys.* **2006**, *125*, 224105.
(39) Rérat, M.; Kirtman, B. First-Principles Calculation of the Optical Rotatory Power of Periodic Systems: Application on α-Quartz, Tartaric Acid Crystal, and Chiral (n, m)-Carbon Nanotubes. *J. Chem. Theory. Comput.* **2021**, *17*, 4063−4076.
(40) Balduf, T.; Caricato, M. Derivation and implementation of the optical rotation tensor for chiral crystals. *J. Chem. Phys.* **2022**, *157*, 214105.
(41) Desmarais, J. K.; Kirtman, B.; Rérat, M. First-principles calculation of the optical rotatory power of periodic systems: Modern theory with modern functionals. *Phys. Rev. B* **2023**, *107*, 224430.
(42) Moscowitz, A. Theoretical aspects of optical activity part one: small molecules. *Adv. Chem. Phys.* **1962**, *4*, 67−112.


https://doi.org/10.1021/acs.jpca.3c08095
J. Phys. Chem. A 2024, 128, 1197−1206

(43) Moffitt, W.; Moscowitz, A. Optical activity in absorbing media. *J. Chem. Phys.* **1959**, *30*, 648−660.
(44) Krykunov, M.; Kundrat, M. D.; Autschbach, J. Calculation of circular dichroism spectra from optical rotatory dispersion, and vice versa, as complementary tools for theoretical studies of optical activity using time-dependent density functional theory. *J. Chem. Phys.* **2006**, *125*, 194110.
(45) Ugras, T. J.; Yao, Y.; Robinson, R. D. Can we still measure circular dichroism with circular dichroism spectrometers: The dangers of anisotropic artifacts. *Chirality* **2023**, *35*, 846−855.
(46) Zinna, F.; Pescitelli, G.; Di Bari, L. Circularly polarized light at the mirror: Caveats and opportunities. *Chirality* **2020**, *32*, 765−769.
(47) Castiglioni, E.; Biscarini, P.; Abbate, S. Experimental aspects of solid state circular dichroism. *Chirality* **2009**, *21*, E28−E36.
(48) Castiglioni, E.; Abbate, S.; Longhi, G. Revisiting with Updated Hardware an Old Spectroscopic Technique: Circularly Polarized Luminescence. *Appl. Spectrosc.* **2010**, *64*, 1416−1419.
(49) Pescitelli, G. ECD exciton chirality method today: a modern tool for determining absolute configurations. *Chirality* **2022**, *34*, 333−363.
(50) Bertocchi, F.; Sissa, C.; Painelli, A. Circular dichroism of molecular aggregates: A tutorial. *Chirality* **2023**, *35*, 681−691.
(51) Fortino, M.; Schifino, G.; Pietropaolo, A. Simulation workflows to predict the circular dichroism and circularly polarized luminescence of chiral materials. *Chirality* **2023**, *35*, 673−680.
(52) Jurinovich, S.; Pescitelli, G.; Di Bari, L.; Mennucci, B. A TDDFT/MMPol/PCM model for the simulation of exciton-coupled circular dichroism spectra. *Phys. Chem. Chem. Phys.* **2014**, *16*, 16407−16418.
(53) Padula, D.; Jurinovich, S.; Di Bari, L.; Mennucci, B. Simulation of Electronic Circular Dichroism of Nucleic Acids: From the Structure to the Spectrum. *Chem.—Eur. J.* **2016**, *22*, 17011−17019.
(54) Loco, D.; Jurinovich, S.; Bari, L. D.; Mennucci, B. A fast but accurate excitonic simulation of the electronic circular dichroism of nucleic acids: how can it be achieved? *Phys. Chem. Chem. Phys.* **2016**, *18*, 866−877.
(55) Chang, Y.-W.; Jin, B.-Y. Polarized excitons and optical activity in single-wall carbon nanotubes. *Phys. Rev. B* **2018**, *97*, 205413.
(56) Bradley, D. F.; Tinoco, I., Jr.; Woody, R. W. Absorption and rotation of light by helical oligomers: The nearest neighbor approximation. *Biopolymers* **1963**, *1*, 239−267.
(57) Tinoco, I., Jr; Woody, R. W. Optical rotation of oriented helices. IV. A free electron on a helix. *J. Chem. Phys.* **1964**, *40*, 160−165.
(58) Wang, X.; Yan, Y. Optical activity of solids from first principles. *Phys. Rev. B* **2023**, *107*, 045201.
(59) Hirata, S.; Head-Gordon, M.; Bartlett, R. J. Configuration interaction singles, time-dependent Hartree−Fock, and time-dependent density functional theory for the electronic excited states of extended systems. *J. Chem. Phys.* **1999**, *111*, 10774−10786.
(60) Bussy, A.; Hutter, J. Efficient and low-scaling linear-response time-dependent density functional theory implementation for core-level spectroscopy of large and periodic systems. *Phys. Chem. Chem. Phys.* **2021**, *23*, 4736−4746.
(61) Kronik, L.; Neaton, J. B. Excited-State Properties of Molecular Solids from First Principles. *Annu. Rev. Phys. Chem.* **2016**, *67*, 587−616.
(62) Izmaylov, A. F.; Scuseria, G. E. Why are time-dependent density functional theory excitations in solids equal to band structure energy gaps for semilocal functionals, and how does nonlocal Hartree−Fock-type exchange introduce excitonic effects? *J. Chem. Phys.* **2008**, *129*, 034101.
(63) Webster, R.; Bernasconi, L.; Harrison, N. M. Optical properties of alkali halide crystals from all-electron hybrid TD-DFT calculations. *J. Chem. Phys.* **2015**, *142*, 214705.
(64) Lorenz, M.; Usvyat, D.; Schütz, M. Local *ab initio* methods for calculating optical band gaps in periodic systems. I. Periodic density fitted local configuration interaction singles method for polymers. *J. Chem. Phys.* **2011**, *134*, 094101.
(65) Iannuzzi, M.; Chassaing, T.; Wallman, T.; Hutter, J. Ground and Excited State Density Functional Calculations with the Gaussian and Augmented-Plane-Wave Method. *Chimia* **2005**, *59*, 499.
(66) Hehn, A.-S.; Sertcan, B.; Belleflamme, F.; Chulkov, S. K.; Watkins, M. B.; Hutter, J. Excited-State Properties for Extended Systems: Efficient Hybrid Density Functional Methods. *J. Chem. Theory Comput.* **2022**, *18*, 4186−4202.
(67) Strand, J.; Chulkov, S. K.; Watkins, M. B.; Shluger, A. L. First principles calculations of optical properties for oxygen vacancies in binary metal oxides. *J. Chem. Phys.* **2019**, *150*, 044702.
(68) Lorenz, M.; Maschio, L.; Schütz, M.; Usvyat, D. Local *ab initio* methods for calculating optical bandgaps in periodic systems. II. Periodic density fitted local configuration interaction singles method for solids. *J. Chem. Phys.* **2012**, *137*, 204119.
(69) Ochi, M.; Tsuneyuki, S. Optical Absorption Spectra Calculated from a First-Principles Wave Function Theory for Solids: Trans-correlated Method Combined with Configuration Interaction Singles. *J. Chem. Theory Comput.* **2014**, *10*, 4098−4103.
(70) Ketolainen, T.; Macháčová, N.; Karlický, F. Optical Gaps and Excitonic Properties of 2D Materials by Hybrid Time-Dependent Density Functional Theory: Evidences for Monolayers and Prospects for van der Waals Heterostructures. *J. Chem. Theory Comput.* **2020**, *16*, 5876−5883.
(71) Bannwarth, C.; Grimme, S. Electronic Circular Dichroism of Highly Conjugated $\pi$-Systems: Breakdown of the Tamm−Dancoff/Configuration Interaction Singles Approximation. *J. Phys. Chem. A* **2015**, *119*, 3653−3662.
(72) Krukau, A. V.; Vydrov, O. A.; Izmaylov, A. F.; Scuseria, G. E. Influence of the exchange screening parameter on the performance of screened hybrid functionals. *J. Chem. Phys.* **2006**, *125*, 224106.
(73) Parsons, T.; Balduf, T.; Cheeseman, J. R.; Caricato, M. Basis Set Dependence of Optical Rotation Calculations with Different Choices of Gauge. *J. Phys. Chem. A* **2022**, *126*, 1861−1870.
(74) Bernasconi, L.; Webster, R.; Tomić, S.; Harrison, N. M. Optical response of extended systems from time-dependent Hartree-Fock and time-dependent density-functional theory. *J. Phys.: Conf. Ser.* **2012**, *367*, 012001.
(75) Ferrari, A. M.; Orlando, R.; Rérat, M. *Ab Initio* Calculation of the Ultraviolet−Visible (UV-vis) Absorption Spectrum, Electron-Loss Function, and Reflectivity of Solids. *J. Chem. Theory Comput.* **2015**, *11*, 3245−3258.
(76) Sander, T.; Maggio, E.; Kresse, G. Beyond the Tamm-Dancoff approximation for extended systems using exact diagonalization. *Phys. Rev. B* **2015**, *92*, 045209.
(77) Kolos, M.; Karlický, F. Accurate many-body calculation of electronic and optical band gap of bulk hexagonal boron nitride. *Phys. Chem. Chem. Phys.* **2019**, *21*, 3999−4005.
(78) Pescitelli, G.; Di Bari, L.; Berova, N. Conformational aspects in the studies of organic compounds by electronic circular dichroism. *Chem. Soc. Rev.* **2011**, *40*, 4603−4625.
(79) Beran, G. J. O. Modeling Polymorphic Molecular Crystals with Electronic Structure Theory. *Chem. Rev.* **2016**, *116*, 5567−5613.
(80) London, F. Théorie Quantique Des Courants Interatomiques Dans Les Combinaisons Aromatiques. *J. Phys. Radium* **1937**, *8*, 397−409.
(81) Caricato, M. Origin invariant optical rotation in the length dipole gauge without London atomic orbitals. *J. Chem. Phys.* **2020**, *153*, 151101.
(82) Caricato, M.; Balduf, T. Origin invariant full optical rotation tensor in the length dipole gauge without London atomic orbitals. *J. Chem. Phys.* **2021**, *155*, 024118.
(83) Niemeyer, N.; Caricato, M.; Neugebauer, J. Origin invariant electronic circular dichroism in the length dipole gauge without London atomic orbitals. *J. Chem. Phys.* **2022**, *156*, 154114.
(84) Zinna, F.; Di Bari, L. Lanthanide Circularly Polarized Luminescence: Bases and Applications. *Chirality* **2015**, *27*, 1−13.
(85) Gorecki, M.; Carpita, L.; Arrico, L.; Zinna, F.; Di Bari, L. Chiroptical methods in a wide wavelength range for obtaining Ln 3+ complexes with circularly polarized luminescence of practical interest. *Dalton Trans* **2018**, *47*, 7166−7177.
(86) Gendron, F.; Moore, B., II; Cador, O.; Pointillart, F.; Autschbach, J.; Le Guennic, B. Ab Initio Study of Circular Dichroism and Circularly


https://doi.org/10.1021/acs.jpca.3c08095
J. Phys. Chem. A 2024, 128, 1197−1206

Polarized Luminescence of Spin-Allowed and Spin-Forbidden Transitions: From Organic Ketones to Lanthanide Complexes. *J. Chem. Theory Comput.* **2019**, *15*, 4140−4155.
(87) Ludowieg, H. D.; Srebro-Hooper, M.; Crassous, J.; Autschbach, J. Optical Activity of Spin-Forbidden Electronic Transitions in Metal Complexes from Time-Dependent Density Functional Theory with Spin-Orbit Coupling. *ChemistryOpen* **2022**, *11*, No. e202200020.
(88) Spano, F. C.; Meskers, S. C. J.; Hennebicq, E.; Beljonne, D. Probing Excitation Delocalization in Supramolecular Chiral Stacks by Means of Circularly Polarized Light: Experiment and Modeling. *J. Am. Chem. Soc.* **2007**, *129*, 7044−7054.



https://doi.org/10.1021/acs.jpca.3c08095
*J. Phys. Chem. A* 2024, 128, 1197−1206